Neuro-Oncology

24(8), 1352–1363, 2022 | https://doi.org/10.1093/neuonc/noab299 | Advance Access date 4 January 2022

Liquid biopsy detection of genomic alterations in pediatric brain tumors from cell-free DNA in peripheral blood, CSF, and urine

Mélanie Pagès, Denisse Rotem, Gregory Gydush, Sarah Reed, Justin Rhoades, Gavin Ha, Christopher Lo, Mark Fleharty, Madeleine Duran, Robert Jones, Sarah Becker, Michaela Haller, Claire E. Sinai, Liliana Goumnerova, Todd R. Golub, J. Christopher Love, Keith L. Ligon, Karen D. Wright†, Viktor A. Adalsteinsson†, Rameen Beroukhim†, and Pratiti Bandopadhayay†

Dana-Farber/Boston Children's Cancer and Blood Disorders Center, Boston, Massachusetts, USA (M.P., T.R.G., K.L.L., K.D.W., P.B.); GHU-Paris—Sainte-Anne Hospital, Department of Neuropathology, Paris University, Paris, France (M.P.); Broad Institute of Harvard and MIT, Cambridge, Massachusetts, USA (D.R., G.G., S.R., J.R., G.H., C.L., M.F., M.D., T.R.G., K.L.L., V.A.A., R.B., P.B.); Department of Oncologic Pathology, Dana Farber/Brigham and Women's Cancer Center, Boston, Massachusetts, USA (R.J., S.B., M.H., C.E.S.); Department of Neurosurgery, Boston Children's Hospital, Boston, Massachusetts, USA (L.G., K.L.L.); Massachusetts Institute of Technology, Cambridge, Massachusetts, USA (J.C.L., V.A.A.); Department of Medical Oncology, Dana-Farber Cancer Institute, Boston, Massachusetts, USA (R.B.); Department of Medicine, Brigham and Women's Hospital, Boston, Massachusetts, USA (R.B.); Department of Cancer Biology, Dana-Farber Cancer Institute, Boston, Massachusetts, USA (R.B.)

Affiliation when this work was performed: Department of Pediatric Oncology, Dana-Farber Cancer Institute, Boston, Massachusetts, USA (M.P.); GHU-Paris—Sainte-Anne Hospital, Department of Neuropathology, Paris University, Paris, France (M.P.); Broad Institute of Harvard and MIT, Cambridge, Massachusetts, USA (D.R., S.R., G.H., M.D.); Department of Oncologic Pathology, Dana Farber/Brigham and Women's Cancer Center, Boston, Massachusetts, USA (R.J., S.B., M.H., C.E.S.); Department of Neurosurgery, Boston Children's Hospital, Boston, Massachusetts, USA (L.G.)

†These authors contributed equally to this work.

Corresponding Authors: Rameen Beroukhim, MD, PhD, Dana-Farber Cancer Institute, 450 Brookline Ave, Boston, MA 02115, USA (rameen_beroukhim@dfci.harvard.edu); Pratiti Bandopadhayay, MBBS, PhD, Dana-Farber Cancer Institute, 450 Brookline Ave, Boston, MA 02115, USA (pratiti_bandopadhayay@dfci.harvard.edu); Viktor A. Adalsteinsson, PhD, Broad Institute, 450 Main Street, Cambridge, MA 02142, USA (viktor@broadinstitute.org); Karen Wright, MD, MS, Dana-Farber Cancer Institute, 450 Brookline Ave, Boston, MA 02115, USA (karen_wright@dfci.harvard.edu).

Abstract

Background. The ability to identify genetic alterations in cancers is essential for precision medicine; however, surgical approaches to obtain brain tumor tissue are invasive. Profiling circulating tumor DNA (ctDNA) in liquid biopsies has emerged as a promising approach to avoid invasive procedures. Here, we systematically evaluated the feasibility of profiling pediatric brain tumors using ctDNA obtained from plasma, cerebrospinal fluid (CSF), and urine.

Methods. We prospectively collected 564 specimens (257 blood, 240 urine, and 67 CSF samples) from 258 patients across all histopathologies. We performed ultra-low-pass whole-genome sequencing (ULP-WGS) to assess copy number variations and estimate tumor fraction and developed a pediatric CNS tumor hybrid capture panel for deep sequencing of specific mutations and fusions.

Results. ULP-WGS detected copy number alterations in 9/46 (20%) CSF, 3/230 (1.3%) plasma, and 0/153 urine samples. Sequencing detected alterations in 3/10 (30%) CSF, 2/74 (2.7%) plasma, and 0/2 urine samples. The only positive results were in high-grade tumors. However, most samples had insufficient somatic mutations (median 1, range 0-39) discoverable by the sequencing panel to provide sufficient power to detect tumor fractions of greater than 0.1%.

Conclusions. Children with brain tumors harbor very low levels of ctDNA in blood, CSF, and urine, with CSF having the most DNA detectable. Molecular profiling is feasible in a small subset of high-grade tumors. The level of clonal aberrations per genome is low in most of the tumors, posing a challenge for detection using whole-genome or even targeted sequencing methods. Substantial challenges therefore remain to genetically characterize pediatric brain tumors from liquid biopsies.

Key Points

- The use of ctDNA for molecular profiling of pediatric CNS tumors is feasible in a restricted subset of patients.
- Analysis of false-positive rates of methods developed to detect ctDNA is mandatory due to high rates of sequencing artifacts.

Importance of the Study

We present the largest prospective analysis of the utility of cell-free DNA (cfDNA) detection for children with primary brain tumors across all histological subtypes and systematically evaluate the sensitivity and specificity of our approaches. Our results demonstrate that the detection of circulating tumor DNA (ctDNA) is limited in the majority of children with brain tumors by low yields of cfDNA and a paucity of genomic alterations that can be detected by sequencing assays. Moreover, we find a high rate of false-positive results, highlighting the necessity to carefully determine the sensitivity and specificity of assays developed to detect ctDNA in children with brain tumors. We find that substantial challenges currently limit the clinical utility of ctDNA detection in the majority of children diagnosed with pediatric brain tumors.

The analysis of circulating tumor DNA (ctDNA) has rapidly emerged as a noninvasive alternative to molecular testing[1–4] to facilitate precision medicine approaches. Similar approaches in pediatric neurooncology, however, face major challenges, largely due to low burdens of ctDNA relative to that associated with extra-cranial cancers.[5] Compared to adult cancers, pediatric tumors often harbor "quiet" cancer genomes with fewer somatic genetic alterations to detect.[6]

Here, we assessed the feasibility of ctDNA collection and assessment using methodologies tailored to detect ctDNA from pediatric brain tumors over 500 liquid biopsies (cerebrospinal fluid [CSF], plasma, and/or urine) from more than 250 children with primary central nervous system (CNS) tumors.

Materials and Methods

Patient Cohort and Sample Processing

Pediatric patients with primary CNS tumors over a 2-year period from the Dana-Farber Cancer Institute/Boston Children's Hospital were prospectively identified.

Venous blood (1-10 mL) and CSF were collected in Streck Cell-Free DNA BCT collection tubes (Streck Inc., Omaha, NE, USA) or Vacutainer EDTA tubes (Becton Dickinson, Oakville, ON, Canada). Tubes were either processed within 4 hours of collection or stored at 4°C and processed within 24 hours. Whole blood was centrifuged at 1900*g* for 10 minutes. After discarding the red blood cells, plasma was centrifuged a second time at 15 000*g* for 10 minutes in low-bind tubes to remove residual cells from plasma. The supernatant was then frozen at –80°C until ready for further processing. Germline DNA was extracted from corresponding buffy coats.

Urine was collected in a sterile collection cup and either stored at 4°C for less than 2 hours or urine preservative was added (10%-20% volume of Streck Cell-Free DNA urine preservative) for storage at room temperature for up to 24 hours. Urine was then centrifuged as described above.

Between 0.5-1 mL CSF was collected in Streck Cell-Free DNA BCT (Streck Inc., Omaha, NE, USA) or in a sterile collection tube and stored at either room temperature or 4°C. CSF was centrifuged within 24 hours of collection (or 2 hours if no preservative) at 1900*g* for 10 minutes at room temperature and then the supernatant was collected and stored at –80°C.

DNA Extraction and Sequencing

Cell-free DNA (cfDNA) was extracted using the Qiagen Circulating DNA kit (Qiagen, Hilden, Germany) and quantified using the PicoGreen assay on a Hamilton STAR-line liquid handling system. Sequencing libraries were constructed from cfDNA input ranging from 5 to 50 ng using a Kapa Hyper Prep kit and short duplex adapters (IDT, Coralville, IA, USA and Broad Institute) as previously described.[7]

A total of 5-20 ng of cfDNA input was used for ultra-low-pass whole-genome sequencing (ULP-WGS). Sequencing

libraries were pooled and sequenced using 100-bp paired-end runs over 1× lane on a HiSeq 2500 (Illumina, San Diego, CA, USA) to an average genome-wide fold coverage of 0.1×.

Hybrid capture sequencing on germline DNA and cfDNA was performed using solution-based hybrid selection (IDT lockdown protocol) and biotinylated 80 bp DNA probes designed by Illumina and synthesized by Twist Bioscience. Libraries were sequenced using 150 bp paired-end runs on an Illumina HiSeq 4000 with a targeted coverage of 10 000×, using a targeted panel designed to cover loci where alterations have been detected in pediatric brain tumors (Supplementary Table 1).

Genomic Analyses

Copy number alterations (CNAs) and mutations in tumors were identified from OncoPanel sequencing data or OncoCopy microarray data generated in the course of clinical care[6] (Supplementary Table 2). OncoPanel is a targeted sequencing panel that includes 300 cancer-related genes and 113 introns over 35 genes for the detection of rearrangements.[8] OncoCopy is an array CGH platform with a resolution of 2.1 kb across the genome.[9]

Tumor fractions (TF) from ULP-WGS were estimated using ichorCNA.[7] ichorCNA determines read counts per 1 Mb bins across the genome and normalizes them to correct for GC-content biases and gender effects on chromosomes X and Y. It then feeds these into a Hidden Markov Model, whose parameters are determined using a Bayesian statistical framework, to estimate both TF and copy number states across the genome.

Pairwise sample comparisons were carried out using Pearson correlations. To account for experimental artifacts (back noise in coverage data that could be interpreted as CNA), we used a more stringent test that the cfDNA copy number profile should be correlated with its matched tumor to a greater degree than to unmatched tumors. We therefore determined the threshold for significant correlation to be $r = 0.41$ by comparing copy number levels from all cfDNA samples against copy number levels from all non-matched tumors. r values that were above 0.41 were only observed in >5% of these control comparisons (ie, $P = .05$). We also visually examined the similarity between every copy number profile generated from ULP-WGS with the matched tumor profile.

CNAs were called from hybrid capture sequencing data using GATK on Firecloud. Somatic mutations were called using duplex consensus called bams produced by our pipeline that incorporates duplex unique molecular identifiers (UMI). Custom analytical scripts were used to identify unique families of parental molecules in the originating samples based on the UMIs. This pipeline makes use of UMIs for increasing the available depth of reads and reduces error. Somatic mutations were identified as sequences that did not match the germline reference, were shared among all reads with the same duplex unique molecular identifiers, and were also mutated in the paired tumor. All candidate somatic mutations and structural alterations including CNAs were manually reviewed using the Integrative Genomics Viewer.[10]

Plots were generated using the ggplot2 package in R (v.3.4.3) and Prism (v.8.2.1). All statistical analyses were performed in R (v.3.4.3).

Ethics Statement

Patients were enrolled after informed consent under IRB-approved Dana-Farber Cancer Institute protocol N° 10-417.

Results

Systematic Processing of cfDNA in Pediatric Primary CNS Tumor Patients

We prospectively collected 564 liquid biopsies from 258 pediatric patients who were evaluated for a primary pediatric CNS tumor. These samples were processed and analyzed as depicted in Figure 1A. The cohort encompassed over 13 tumor types (Figure 1B; Supplementary Table 2), primarily low-grade gliomas or glioneuronal tumors (LGGs or LGNTs; n = 102), high-grade gliomas or glioneuronal tumors (HGGs or HGNTs, n = 35), and embryonal tumors including medulloblastomas (n = 27), atypical teratoid/rhabdoid tumors (AT/RTs, n = 5), and others (n = 7).

The samples consisted of 67 CSF samples from 54 patients, 257 plasma samples from 243 patients, and 240 urine samples from 224 patients. We obtained more than one of these samples from 227 patients (Figure 1C; Supplementary Table 2). For 139 patients, CSF, blood, or urine was collected prior to tumor resection; for 33 patients we obtained these samples during or within 24 hours of surgery; and for 86 patients, we obtained these samples at subsequent time points. Ninety-one samples were obtained at recurrence. Across all samples, 225 were collected prior to or immediately after tumor resection (Supplementary Table 2).

We extracted cfDNA from 509 CSF, plasma, and urine samples using methodologies that we had previously established (see Methods). This yielded a median of 18.3 nanograms of DNA (6.4 ng from CSF, 20.9 ng from plasma, and 15.5 ng from urine; range 0-3043; Supplementary Figure 1A–C; Supplementary Table 2), with a median fragment size of 169.7 base pairs (Supplementary Figure 2).

ULP-WGS for Copy Number Detection in ctDNA

We and others have previously used ULP-WGS to detect large-scale CNAs and estimate TF in cfDNA.[7] We therefore sought to determine whether ULP-WGS could uncover high levels of tumor DNA (eg, >10%) in plasma, CSF, or urine samples from patients such that copy number analysis could be done non-invasively. However, many CNS tumors in children harbor few or no large-scale CNAs, and CNS tumors in both children and adults have been associated with low fractions of ctDNA.

We successfully constructed ULP-WGS libraries and obtained evaluable sequencing data for 429 samples (84% of the processed cfDNA samples) from 240 patients (46 CSF, 230 plasma, and 153 urine samples) (Supplementary Table 2).

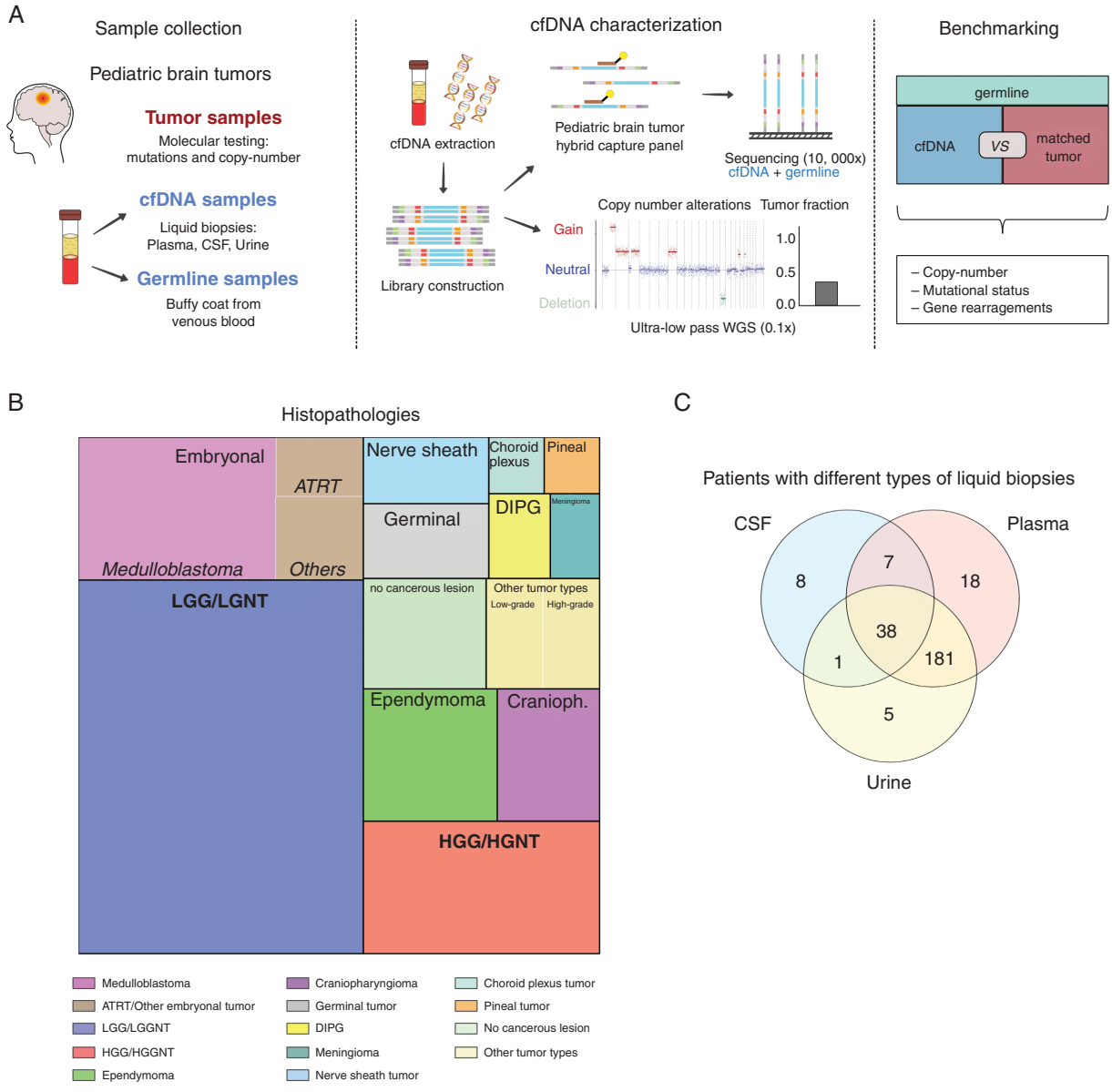

Fig. 1 cfDNA sample collection. (A) Workflow. (B) Histopathological diagnoses of the tumors included in the cohort. (C) Types of liquid biopsies collected for the 251 patients. Abbreviation: cfDNA, cell-free DNA.

Across all plasma samples, we detected low amounts of ctDNA in our cohort applying the ichorCNA algorithm.[7] The TF was estimated to be above 10% in only 5 samples (2%) (4 patients from patients with a high-grade tumor and 1 patient with a LGG) (Supplementary Table 2) with a median TF estimation of 0.9% (range 0%-98%). Matched tumor copy number data were available for 132 plasma samples and concordance was found for 3 samples (Supplementary Table 2) with TF estimation of 4.9%, 3.5%, and 2.7%.

As an alternative approach taking advantage of matched tumor data (which ichorCNA does not have) to get to lower TF, we examined the similarity between the 261 copy number profiles generated from ULP-WGS of cfDNA with their matched tumor data (Figure 2A). Among the 240 patients with ULP-WGS data, copy number profiles of the matched tumors were available for 132 tumors corresponding to 261 cfDNA samples (31 CSF, 132 plasma, and 98 urine). Only 78/132 (59%) samples exhibited at least one CNA at a chromosome arm level (chromosome arm gain or loss) (Figure 2B) in the bulk tumor biopsies.

We first performed a systematic Pearson correlation analysis of the 261 cfDNA samples vs their 132 matched tumors. Our previous analyses had shown that CNA detection is most reliable when TF is above 0.10.[7] We determined the threshold for significant correlation at $r = 0.41$ for $P = .05$ by computing copy number levels from all cfDNA samples against copy number levels from all non-matched tumors. Examples of copy number profiles from paired

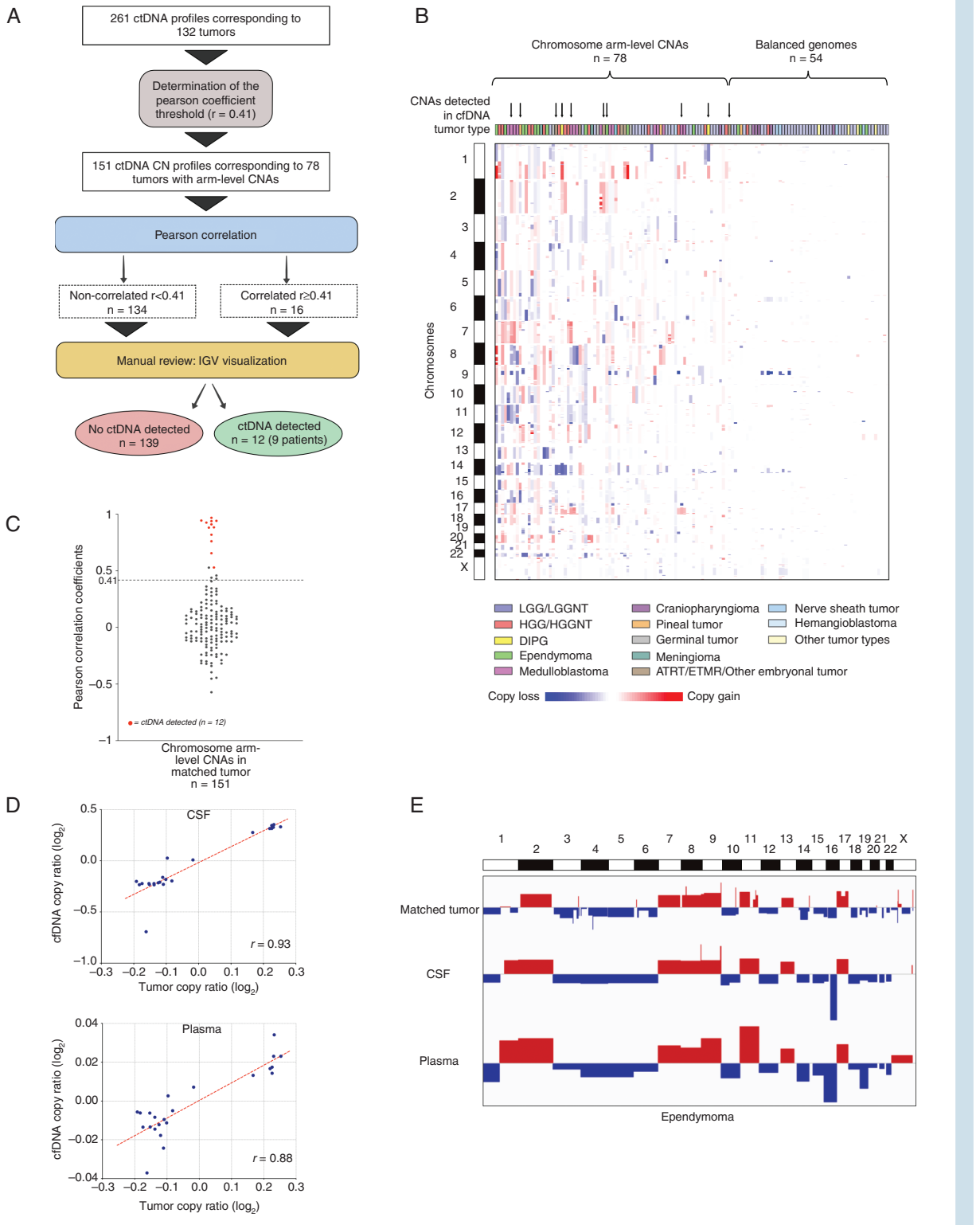

Fig. 2 ULP-WGS for copy number detection in cfDNA. (A) Analysis method to compare copy number profiles of cfDNA samples to those of their matched tumors. (B) Copy number profiles in the tumors of 132 patients with matched cfDNA. Gains are in red and losses are in blue. (C) Pearson correlation coefficients from the copy number comparison. The dotted line indicates the threshold for a statistically significant correlation. Samples with detected ctDNA are highlighted in red. (D) Copy number ratios from a single tumor (horizontal axis) against the copy number ratios from cfDNA from paired CSF (top) and plasma (bottom). *r* represents the Pearson correlation coefficient. (E) Genome-wide copy number profiles of DNA obtained from the tumor, CSF, and plasma from panel D. Gains are in red and losses are in blue. Abbreviations: cfDNA, cell-free DNA; CSF, cerebrospinal fluid; ctDNA, circulating tumor DNA; ULP-WGS, ultra-low-pass whole-genome sequencing.

cfDNA and tumor samples with a range of *r* values (0.007-0.9) are shown in Supplementary Figure 3.

We then performed a Pearson correlation on 151 cfDNA samples and their 78 matched tumors that exhibited at least one CNA at a chromosome arm level (chromosome arm gain or loss). We obtained positive correlations for only 16 samples (10.6%). After manual review, four samples were not clearly conclusive (*r* range [0.43-0.53]), leaving 12 positive samples, obtained from 9 patients, including 9 CSF and 3 plasma samples (no positive urine sample) (Figure 2A and C; Supplementary Tables 2 and 3).

The histological diagnoses that yielded positive results comprised only WHO grade III and IV tumors, including 3 medulloblastomas, 1 pineoblastoma, 1 ependymoma, 2 embryonal tumors, and 2 DIPGs (Supplementary Figure 4; Supplementary Table 3). An example of positive CSF samples from two time points and a positive plasma sample from a patient with ependymoma is shown in Figure 2D and E.

We validated the low rates of detection of ctDNA in our cohort by applying an orthogonal approach. Our team has previously developed ichorCNA has a method to detect ctDNA, which we have extensively validated to be sufficient to reliably detect CNAs in tumor-derived DNA present at thresholds of at least 10%.[7] Among the 12 samples that we had deemed to be positive for ctDNA because of matching copy number profiles with matched tumors, ichorCNA classified nine as having more than 10% tumor DNA. Among the other 249 samples, ichorCNA classified only 7 as having more than 10% ctDNA.

Taken together, these results suggest low levels of ctDNA detection in samples obtained from children with primary brain tumors.

Design and Validation of a Hybrid Capture Sequencing Panel

We next evaluated whether we could improve ctDNA detection by interrogating point mutations, rearrangements, and copy number events using a hybrid capture panel designed to cover mutation hotspots in pediatric CNS tumors. We initially identified all genes that had been reported to harbor mutations or rearrangements to a statistically significant level within 25 published cohorts of pediatric CNS tumors.[11–35] This survey initially generated a list of 91 genes (Supplementary Table 1, panel V1); we included 46 of these genes that were most frequently mutated and were predicted to have the highest specificity for capturing on-target DNA (Supplementary Table 1, panel V2). Using DNA mixing experiments (we used two healthy donors; one was spiked into the other one to create our benchmark samples at 1 pct, 2.5 pct, and 5 pct. This provided us with 0.5 pct, 1.25 pct, and 2.5 pct allele fraction variants) and sequencing to 10 000× average depth at the covered bases, we found that this assay provided a sensitivity above 80% for the detection of a single-nucleotide variant (SNV) at an allele fraction above 0.01% (Supplementary Figure 5) and 70% for the detection of a structural variant (SV) at an allele fraction above 0.5% (Supplementary Figure 6).

Hybrid Capture Sequencing for ctDNA Detection in Low-Purity or Diploid Samples

We applied this panel to 86 cfDNA samples from 75 patients, comprising 10 CSF, 74 plasma, and 2 urine samples, along with their germline DNA. Among this cohort, 28 samples were collected at least 24 hours after surgical resection, with gross residual tumor present in 22 of these 28 patients. This sample set was chosen to enrich for high-grade tumors (47% of those sequenced) which harbor a larger number of copy number or mutations. Nevertheless, our first determination was that, despite covering the most commonly altered sites in pediatric CNS tumors, tumors from only 42 of these patients, corresponding to 47 samples, harbored somatic genetic SNVs or rearrangements that could be called by our capture panel (Figure 3A), with a median of 1 mutation per primary tumor overall. The 42 remaining tumors harbored from 1 to 39 callable events, for a total of 95 somatic SNVs and 11 somatic rearrangements across the cohort. Given these findings, we conclude that alternate panel designs will be required to achieve high levels of sensitivity for ctDNA from pediatric CNS tumors.

Occasional Matches in Raw Reads Reflect False-Positives

Prior studies have reported detection of somatic variants from deep targeted sequencing based on single reads that have not been error corrected. We first evaluated whether the accuracy of this approach.

We initially focused on evaluating 88 mutations found in 34 tumors and manually reviewed sequence reads at corresponding loci in the cfDNA samples. Using this approach, we found cfDNA reads with the appropriate mutation in 56 cases (64%). The average allelic fraction (AF) of these mutations was 0.15%. We also evaluated 11 rearrangements in 11 tumors but did not detect cfDNA reads corresponding to any of these rearrangements.

To determine the extent to which these apparent positive results reflect sequencing artifact rather than true alterations in ctDNA, we examined negative controls. Specifically, we selected 6 loci for which no mutation was detected across our 75 tumors and evaluated the cfDNA corresponding to 8 of those tumors at each of these loci (48 cfDNA locus pairs examined). We detected individual positive mutation reads in 32/48 (67%) of these locus cfDNA pairs, with an average AF of 0.08%. These AF rates are similar to the rates at which we detected true tumor-specific mutations in individual reads in cfDNA. We conclude that assessing individual reads at pre-selected loci results in high false-positive rates. We extended this analysis to four glioma hotspot driver mutations: H3F3A K27M, HIST1H3B K27M, IDH1R132H, and BRAFV600E in two cfDNA samples from tumors that were wildtype for these genes. Both of these tumors were of types (one medulloblastoma and one AT/RT) that rarely harbor these mutations. Consistent with our prior analyses, we found these samples to also harbor five mutation reads that were false-positives (5 out of 8 alleles were positive, 63%). When we looked for individual positive reads at

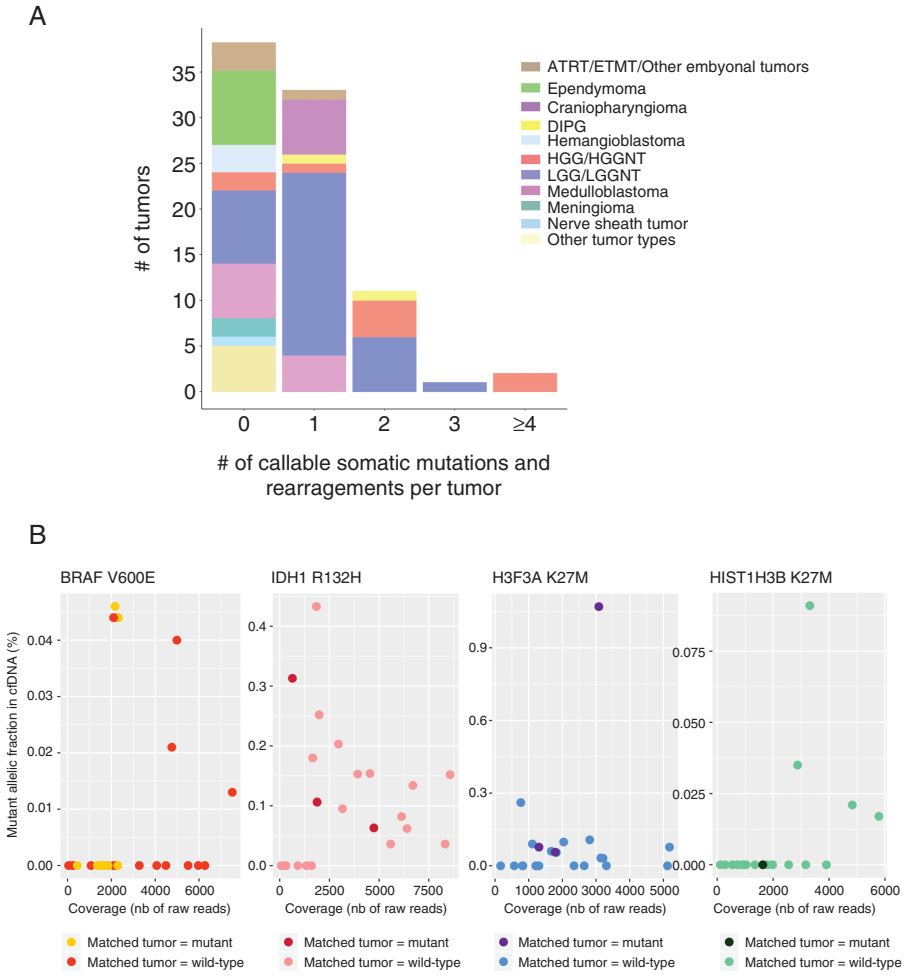

Fig. 3 Hybrid capture sequencing for ctDNA detection—raw-reads analysis. (A) Number of callable mutations and rearrangements detected per primary tumor. (B) Occasional matches in raw reads reflect false-positives. Mutant allelic fraction in raw reads at four glioma hotspot mutation positions (BRAF V600E, IDH1 R132H, H3F3A K27M, HIST1H3B K27M) in cfDNA samples from 22 patients diagnosed with gliomas. Abbreviations: cfDNA, cell-free DNA; ctDNA, circulating tumor DNA.

these four positions in cfDNA samples from all patients with gliomas, we detected a similarly high fraction of likely false-positive reads (Figure 3B).

We conclude that calling mutations based on the presence of individual positive reads compromises specificity to an unacceptable degree due to sequencing artifact.

Standard Analysis of Duplex Reads

To address the issue of false-positive results, we applied a workflow that detected germline variants and callable somatic alterations, including mutations and gene rearrangements, using a pipeline that relies on barcoding DNA fragments prior to amplification to reconstruct double-stranded DNA molecules (the "unique molecular identifier", or UMI, pipeline).[36] The UMIs allowed us to leverage analytical methods that take advantage of duplex reads to improve the sensitivity and specificity of mutation detection in our targeted sequencing analysis below.[37] Moreover, we were able to demonstrate the feasibility to perform ULP-WGS sequencing on these libraries incorporating unique molecular identifiers (UMI).

We then restricted variant calls to alterations that are present in both DNA strands, to filter artifacts that affected only reads from one strand.[36] This procedure also enables us to determine the number of DNA fragments contributing at each genomic locus to determine whether we are limited by sequencing depth or DNA yield.

Across the 106 somatically altered genomic loci in our cohort, we obtained a median coverage of 1143 duplex consensus reads per locus. Median of duplex reads at the analyzed somatic point mutation in CSF was 199.5 (range 82-2189) and 1202 (range 34-7886) in plasma. On a per-sample basis (summing across altered loci within each sample), the median coverage of somatically altered bases was 991 duplex consensus reads (range 42-75 353) (Figure 4A). Known mutation points as well as rearrangement breakpoints were manually reviewed in comparison with the matched tumor profile. Among

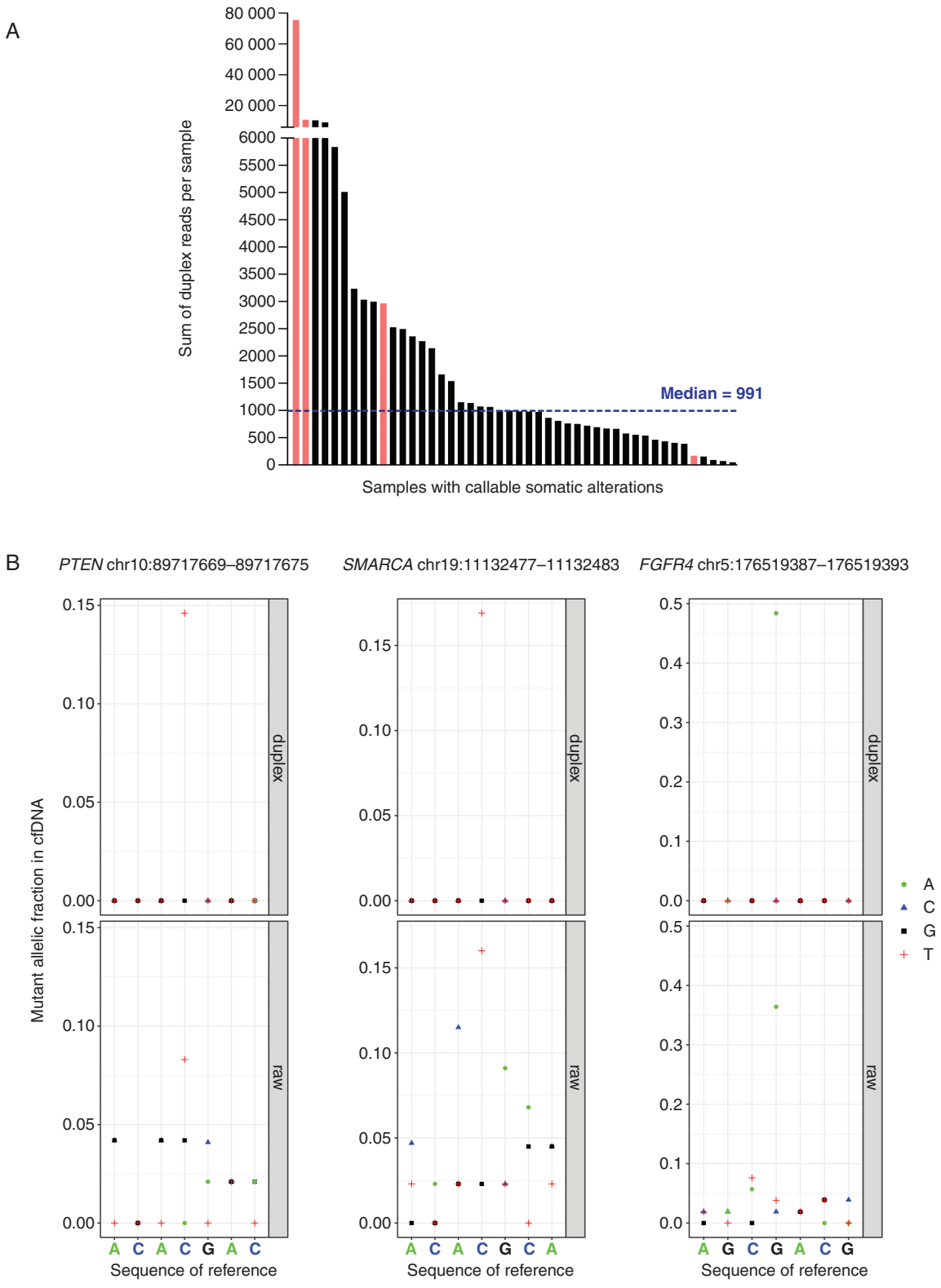

Figure 4. Hybrid capture sequencing for ctDNA detection—duplex-reads analysis. (A) Total number of duplex reads per cfDNA sample. Samples with detected ctDNA are indicated in red. (B) ctDNA detected in a plasma cfDNA sample from a patient diagnosed with an HGG harboring mutations in *PTEN*, *FGFR4*, and *SMARCA4*. Comparison of the mutant allelic fractions between duplex (top panels) and raw reads (bottom panels) at each mutation locus indicates the level of background noise when using raw reads. Abbreviations: cfDNA, cell-free DNA; ctDNA, circulating tumor DNA; HGG, high-grade glioma.

the 106 mutation points analyzed, we detected 7 mutations in ctDNA from 4 patients, all presenting with HGG (Figure 4A; Supplementary Figure 7; Supplementary Table 4). The median mutant allele fraction (MAF) of these somatic variants was 0.48% (range 0.07%-4%). None of the gene fusions identified in matched tumors (n = 11) were detected in cfDNA. Finally, we also analyzed CNAs in 68 samples from 59 patients which allowed us to detect two positive samples. One of these was also detected by ULP-WGS. However, the CNA in the second tumor was a focal homozygous *SMARCB1* deletion (Supplementary Table 3) and therefore not detected by our prior ULP-WGS pipeline which incorporates arm level gains and losses.

Comparison of results obtained by incorporating duplex reads and UMI to those obtained by detecting alterations in single reads highlight the false-positive rate associated with the latter method. Among the 56 cases in which evaluating single reads had detected the presence of a mutation, none were called positive using the UMI pipeline. Moreover, when we extended this analysis to include the four glioma hotspot driver mutations: H3F3A K27M, HIST1H3B K27M, IDH1R132H, and BRAFV600E from the two cfDNA samples with tumors that did not harbor these alterations and that we had used to benchmark specificity of mutation detection in single reads, our UMI approach did not detect any reads suggestive of the presence of any these mutations.

Furthermore, to illustrate the benefit of the UMI pipeline in reducing background error, we compared raw bam files to duplex consensus bam files for one sample at three mutated loci (Figure 4B). Each of these mutations was clearly detected above background error using the UMI pipeline (top panels), but raw-read data exhibited only slightly higher allelic fractions to false-positive mutations in surrounding bases (bottom panels).

Tumor Fraction Is Less Than 1% in Most cfDNA Samples

One use of cfDNA profiling is simply tumor detection. However, detection power is a function of the number of cfDNA molecules per sample tested for potential mutations. Considering most patients only had 1 or 2 tumor mutations within the region targeted in cfDNA, we expected detection power to be limited.

We evaluated this by estimating the maximum tumor purity of our cfDNA samples, given the rates of somatic mutation detection we observed (Figure 5). Specifically, we calculated the probability to detect ctDNA for every patient across a range of TF (0.01%, 0.1%, and 1%). We expected our power to detect ctDNA would scale with the total number of duplex reads encompassing sites with mutations in the tumor (Figure 5, horizontal axis). Note that this scales with both the number of detectable mutations and the number of duplex reads encompassing each mutation. At a 1% TF (blue curve), we estimate >90% power to detect ctDNA across 80% of the patients (vertical lines); however, we detected ctDNA in only four patients (vertical pink lines), indicating that the actual TF were lower than 1% in most cases. Our power to detect a TF of 0.1% (orange curve), was only >50% for 37% of the samples. We conclude that detection of ctDNA from pediatric CNS tumors is limited by low TF in cfDNA and low mutation counts per tumor.

Discussion

The feasibility of detecting ctDNA in plasma or CSF from pediatric patients with primary CNS tumors—across all types of tumors—has not been systematically evaluated in large cohort of children. Indeed, among 12 previously published studies reporting on cfDNA approaches for patients with primary brain tumors, only four focused on pediatric tumors, while another five manuscripts presented combined pediatric and adult patient cohort, and the largest pediatric brain tumor cohort included less than 30 patients (Supplementary Table 5). Moreover, in brain tumors, results have varied, possibly due to limitations in ctDNA circulation due to the blood-brain barrier.[1,3,5,38–45] Our study presents the largest prospective cohort of cfDNA collected from children with CNS tumors across multiple histologies and uses both genome-wide SCNA (somatic copy number alteration) detection through ULP-WGS and hotspot mutation and rearrangement detection through hybrid capture sequencing to 10 000× depth, on a platform previously shown to be highly sensitive and specific in tracking ctDNA in many types of extra-cranial cancers including in patients with minimal residual disease.[2,7,46,47] The low sensitivity rates we detect despite these technical strengths and separate assays for both SNVs and SCNAs indicate the challenges faced in ctDNA detection from pediatric brain tumors.

Although we find that systematically collecting cfDNA and constructing libraries, including labeling of individual duplex molecules, is feasible in a clinical setting, ctDNA detection from pediatric CNS tumors is limited both by the low TF of cfDNA and the small number of detectable somatic genetic events in these tumors. High-grade tumors can harbor both SNVs and SCNAs, and we specifically designed our hybrid sequencing panel to encompass mutations frequently observed in pediatric CNS tumors, covering 40 genes. However, many pediatric brain tumors, particularly LGGs, harbor single rearrangements which were not detected by our panel, despite deep sequencing coverage.

Other groups have reported yields of cfDNA to be higher in CSF than plasma.[41–45] While we also find a higher detection rate in CSF and high-grade tumors, due to higher TF in CSF and more genomic disruption, we report a lower detection rate in CSF than a published cohort of 85 adult gliomas. This could be due to the higher rate of detectable genomic events in adult gliomas.[48] Previous efforts to detect cfDNA in CSF from patients with brain tumors have leveraged methods such as digital droplet PCR to detect histone mutations.[3,49] Further studies are required in pediatric brain tumor patients, encompassing larger numbers of patients and careful determination of sensitivity and specificity rates of targeted

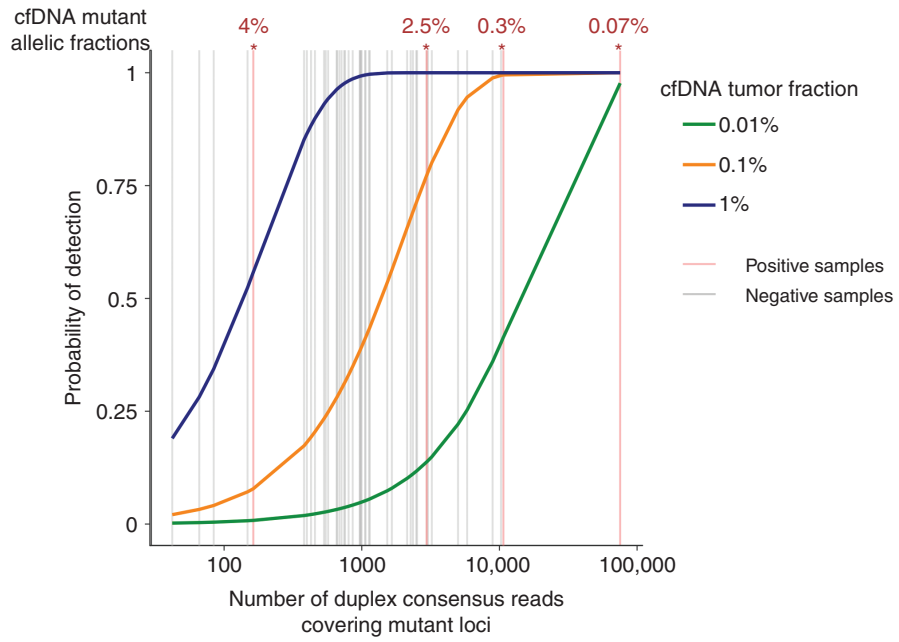

Fig. 5 Probability of detection ctDNA (vertical axis) against the number of cfDNA molecules sequenced (horizontal axis). Only DNA molecules that cover locations found to be mutant in the paired tumor are considered. Detection probabilities are shown for cfDNA tumor fractions of 1%, 0.1%, and 0.01%. Vertical lines represent actual numbers of cfDNA molecules sequenced across samples in this study. Samples for which ctDNA was detected are indicated by red lines; and negative samples are in gray. The observed mutant allelic fractions for the positive cfDNA samples are indicated at the top. Abbreviations: cfDNA, cell-free DNA; ctDNA, circulating tumor DNA.

sequencing panels, focusing in particular false-positive rates, to allow for the determination of the true feasibility of genotyping pediatric high-grade tumors from CSF samples.

Increased power to detect ctDNA would require either collecting more cfDNA or tracking larger numbers of tumor mutations. To increase the number of mutations covered, one could focus on tumors with larger mutation burdens, design patient-specific sequencing panels, or sequence larger fractions of the genome. In the case of low-grade tumors, few mutations exist genome-wide,[6,19,20] limiting the possibilities of improving ctDNA detection in this manner. Moreover, if the intention in profiling cfDNA is to genotype at individually significant loci, either substantially more cfDNA, routine collection of CSF, or a tumor biopsy would be required. However, the collection of more cfDNA is challenging in children, from whom large blood volumes cannot safely be drawn.

Our results highlight methodological challenges in the analysis of cfDNA sequencing results. With such low TF, it is tempting to search for individual reads that suggest the presence of a somatic mutation. However, our results show that such attempts to detect pre-defined alterations in single sequencing reads often result in artifact, and are prone to high false-positive rates unless substantial effort is made to ensure specificity of results, such as by UMI technology to filter out background error.

The systematic use of cfDNA to genotype CNS tumors in children remains problematic with current technologies. This is due to limitations on sensitivity resulting from the low purity of ctDNA in circulating cfDNA, the small numbers of alterations that can be detected, and the small amounts of blood and CSF that can be safely drawn from small children, limiting the amounts of input DNA that are available. Further work is required to overcome these obstacles before assays for ctDNA can be systematically introduced into the clinical setting for children with brain tumors.

Supplementary Material

Supplementary material is available at *Neuro-Oncology* online.

Keywords

circulating tumor DNA | pediatric brain tumors | liquid biopsy | hybrid capture sequencing | ULP-WGS

Acknowledgments

We thank the patients who participated in this study.

Funding

This work was supported by the MIT and Dana-Farber Harvard Cancer Center Bridge Project (C.L., K.D.W, K.L.L., and R.B.), Dana-Farber Cancer Institute Pediatric Low-Grade Glioma Program (K.L., P.B., and R.B.), Nuovo-Soldati Foundation (M.P.), ARC—Association pour la Recherche sur le Cancer (M.P.), Pediatric Brain Tumor Foundation (P.B. and R.B.), National Institute of Health R00CA201592 (P.B.), National Institute of Health R01s CA188228, CA215489, and CA219943 (R.B.), The Gray Matter Brain Cancer Foundation (R.B.), St. Baldricks Foundation (P.B. and R.B.), and Ian's Friends Foundation (R.B.).

Conflict of interest statement. P.B. and R.B. receive grant funding from Novartis Institute of Biomedical Research for an unrelated project. P.B. receives grant funding from Deerfield and consults for QED Therapeutics. R.B. owns equity in Ampressa Therapeutics.

Authorship statement. P.B., R.B., V.A., K.D.W., and K.L. designed the study. R.J., S.B., M.H., C.S., L.G., K.D.W., and T.G. recruited participants. M.P., K.D.W., R.J., S.B., M.H., and C.S. collected the data. M.P., D.R., G.G., S.R., J.R., G.H., C.L., M.F., M.D., and C.L. completed the research and/or analyzed the data. M.P. and M.F. designed the figures. M.P., R.B., and P.B. wrote the manuscript. All authors revised and approved the final manuscript. P.B., R.B., V.A., and K.D.W. supervised the study.

References

1. Zill OA, Banks KC, Fairclough SR, et al. The landscape of actionable genomic alterations in cell-free circulating tumor DNA from 21,807 advanced cancer patients. *Clin Cancer Res.* 2018;24(15):3528–3538.
2. Stover DG, Parsons HA, Ha G, et al. Association of cell-free DNA tumor fraction and somatic copy number alterations with survival in metastatic triple-negative breast cancer. *J Clin Oncol.* 2018;36(6):543–553.
3. Martínez-Ricarte F, Mayor R, Martíinez-Sáez E, et al. Molecular diagnosis of diffuse gliomas through sequencing of cell-free circulating tumor DNA from cerebrospinal fluid. *Clin Cancer Res.* 2018;24(12):2812–2819.
4. Schwaederle M, Husain H, Fanta PT, et al. Detection rate of actionable mutations in diverse cancers using a biopsy-free (blood) circulating tumor cell DNA assay. *Oncotarget.* 2016;7(9):9707–9717.
5. Bettegowda C, Sausen M, Leary RJ, et al. Detection of circulating tumor DNA in early- and late-stage human malignancies. *Sci Transl Med.* 2014;6(224):224ra24.
6. Ramkissoon SH, Bandopadhayay P, Hwang J, et al. Clinical targeted exome-based sequencing in combination with genome-wide copy number profiling: precision medicine analysis of 203 pediatric brain tumors. *Neuro Oncol.* 2017;19(7):986–996.
7. Adalsteinsson VA, Ha G, Freeman SS, et al. Scalable whole-exome sequencing of cell-free DNA reveals high concordance with metastatic tumors. *Nat Commun.* 2017;8(1):1324.
8. Garcia EP, Minkovsky A, Jia Y, et al. Validation of OncoPanel: a targeted next-generation sequencing assay for the detection of somatic variants in cancer. *Arch Pathol Lab Med.* 2017;141(6):751–758.
9. Ramkissoon SH, Bandopadhayay P, Hwang J, et al. Clinical targeted exome-based sequencing in combination with genome-wide copy number profiling: precision medicine analysis of 203 pediatric brain tumors. *Neuro Oncol.* 2017;19(7):986–996.
10. Thorvaldsdóttir H, Robinson JT, Mesirov JP. Integrative Genomics Viewer (IGV): high-performance genomics data visualization and exploration. *Brief Bioinform.* 2013;14(2):178–192.
11. Paugh BS, Zhu X, Qu C, et al. Novel oncogenic PDGFRA mutations in pediatric high-grade gliomas. *Cancer Res.* 2013;73(20):6219–6229.
12. International Cancer Genome Consortium PedBrain Tumor Project. Recurrent MET fusion genes represent a drug target in pediatric glioblastoma. *Nat Med.* 2016;22(11):1314–1320.
13. Wu G, Diaz AK, Paugh BS, et al. The genomic landscape of diffuse intrinsic pontine glioma and pediatric non-brainstem high-grade glioma. *Nat Genet.* 2014;46(5):444–450.
14. Fontebasso AM, Papillon-Cavanagh S, Schwartzentruber J, et al. Recurrent somatic mutations in ACVR1 in pediatric midline high-grade astrocytoma. *Nat Genet.* 2014;46(5):462–466.
15. Zhang L, Chen LH, Wan H, et al. Exome sequencing identifies somatic gain-of-function PPM1D mutations in brainstem gliomas. *Nat Genet.* 2014;46(7):726–730.
16. Jones DTW, Hutter B, Jäger N, et al. Recurrent somatic alterations of FGFR1 and NTRK2 in pilocytic astrocytoma. *Nat Genet.* 2013;45(8):927–932.
17. Zhang J, Wu G, Miller CP, et al. Whole-genome sequencing identifies genetic alterations in pediatric low-grade gliomas. *Nat Genet.* 2013;45(6):602–612.
18. Taylor KR, Mackay A, Truffaux N, et al. Recurrent activating ACVR1 mutations in diffuse intrinsic pontine glioma. *Nat Genet.* 2014;46(5):457–461.
19. Bandopadhayay P, Ramkissoon LA, Jain P, et al. MYB-QKI rearrangements in angiocentric glioma drive tumorigenicity through a tripartite mechanism. *Nat Genet.* 2016;48(3):273–282.
20. Ramkissoon LA, Horowitz PM, Craig JM, et al. Genomic analysis of diffuse pediatric low-grade gliomas identifies recurrent oncogenic truncating rearrangements in the transcription factor MYBL1. *Proc Natl Acad Sci USA.* 2013;110(20):8188–8193.
21. Pages M, Lacroix L, Tauziede-Espariat A, et al. Papillary glioneuronal tumors: histological and molecular characteristics and diagnostic value of SLC44A1-PRKCA fusion. *Acta Neuropathol Commun.* 2015;3:85.
22. Hou Y, Pinheiro J, Sahm F, et al. Papillary glioneuronal tumor (PGNT) exhibits a characteristic methylation profile and fusions involving PRKCA. *Acta Neuropathol.* 2019;137(5):837–846.
23. Wu G, Broniscer A, McEachron TA, et al. Somatic histone H3 alterations in pediatric diffuse intrinsic pontine gliomas and non-brainstem glioblastomas. *Nat Genet.* 2012;44(3):251–253.
24. Schwartzentruber J, Korshunov A, Liu XY, et al. Driver mutations in histone H3.3 and chromatin remodelling genes in paediatric glioblastoma. *Nature.* 2012;482(7384):226–231.
25. Buczkowicz P, Hoeman C, Rakopoulos P, et al. Genomic analysis of diffuse intrinsic pontine gliomas identifies three molecular subgroups and recurrent activating ACVR1 mutations. *Nat Genet.* 2014;46(5):451–456.
26. Pugh TJ, Weeraratne SD, Archer TC, et al. Medulloblastoma exome sequencing uncovers subtype-specific somatic mutations. *Nature.* 2012;488(7409):106–110.
27. Jones DTW, Jäger N, Kool M, et al. Dissecting the genomic complexity underlying medulloblastoma. *Nature.* 2012;488(7409):100–105.
28. Northcott PA, Jones DTW, Kool M, et al. Medulloblastomics: the end of the beginning. *Nat Rev Cancer.* 2012;12(12):818–834.
29. Robinson G, Parker M, Kranenburg TA, et al. Novel mutations target distinct subgroups of medulloblastoma. *Nature.* 2012;488(7409):43–48.

30. Kool M, Jones DTW, Jäger N, et al. Genome sequencing of SHH medulloblastoma predicts genotype-related response to smoothened inhibition. *Cancer Cell.* 2014;25(3):393–405.
31. Morrissy AS, Garzia L, Shih DJH, et al. Divergent clonal selection dominates medulloblastoma at recurrence. *Nature.* 2016;529(7586):351–357.
32. Parker M, Mohankumar KM, Punchihewa C, et al. *C11orf95-RELA* fusions drive oncogenic NF-κB signalling in ependymoma. *Nature.* 2014;506(7489):451–455.
33. Pietsch T, Wohlers I, Goschzik T, et al. Supratentorial ependymomas of childhood carry *C11orf95-RELA* fusions leading to pathological activation of the NF-κB signaling pathway. *Acta Neuropathol.* 2014;127(4):609–611.
34. Pajtler KW, Pfister SM, Kool M. Molecular dissection of ependymomas. *Oncoscience.* 2015;2(10):827–828.
35. Rausch T, Jones DTW, Zapatka M, et al. Genome sequencing of pediatric medulloblastoma links catastrophic DNA rearrangements with TP53 mutations. *Cell.* 2012;148(1–2):59–71.
36. Schmitt MW, Kennedy SR, Salk JJ, et al. Detection of ultra-rare mutations by next-generation sequencing. *Proc Natl Acad Sci USA.* 2012;109(36):14508–14513.
37. Kivioja T, Vähärautio A, Karlsson K, et al. Counting absolute numbers of molecules using unique molecular identifiers. *Nat Methods.* 2011;9(1):72–74.
38. Lavon I, Refael M, Zelikovitch B, Shalom E, Siegal T. Serum DNA can define tumor-specific genetic and epigenetic markers in gliomas of various grades. *Neuro Oncol.* 2010;12(2):173–180.
39. Schwaederle M, Chattopadhyay R, Kato S, et al. Genomic alterations in circulating tumor DNA from diverse cancer patients identified by next-generation sequencing. *Cancer Res.* 2017;77(19):5419–5427.
40. Boisselier B, Gállego Pérez-Larraya J, Rossetto M, et al. Detection of IDH1 mutation in the plasma of patients with glioma. *Neurology.* 2012;79(16):1693–1698.
41. Pan W, Gu W, Nagpal S, Gephart MH, Quake SR. Brain tumor mutations detected in cerebral spinal fluid. *Clin Chem.* 2015;61(3):514–522.
42. Wang Y, Springer S, Zhang M, et al. Detection of tumor-derived DNA in cerebrospinal fluid of patients with primary tumors of the brain and spinal cord. *Proc Natl Acad Sci USA.* 2015;112(31):9704–9709.
43. Mattos-Arruda LD, Mayor R, Ng CKY, et al. Cerebrospinal fluid-derived circulating tumour DNA better represents the genomic alterations of brain tumours than plasma. *Nat Commun.* 2015;6:8839.
44. Pentsova EI, Shah RH, Tang J, et al. Evaluating cancer of the central nervous system through next-generation sequencing of cerebrospinal fluid. *J Clin Oncol.* 2016;34(20):2404–2415.
45. Huang TY, Piunti A, Lulla RR, et al. Detection of histone H3 mutations in cerebrospinal fluid-derived tumor DNA from children with diffuse midline glioma. *Acta Neuropathol Commun.* 2017;5(1):28.
46. Choudhury AD, Werner L, Francini E, et al. Tumor fraction in cell-free DNA as a biomarker in prostate cancer. *JCI Insight.* 2018;3(21):e122109.
47. Parsons HA, Rhoades J, Reed SC, et al. Sensitive detection of minimal residual disease in patients treated for early-stage breast cancer. *Clin Cancer Res.* 2020;26(11):2556–2564.
48. Miller AM, Shah RH, Pentsova EI, et al. Tracking tumour evolution in glioma through liquid biopsies of cerebrospinal fluid. *Nature.* 2019;565(7741):654–658.
49. Mueller S, Jain P, Liang WS, et al. A pilot precision medicine trial for children with diffuse intrinsic pontine glioma-PNOC003: a report from the Pacific Pediatric Neuro-Oncology Consortium. *Int J Cancer.* 2019;145(7):1889–1901.